*Send Orders for Reprints to reprints@benthamscience.ae*





# The Mechanical Property of Bidirectional Geogrid and its Application Research in Retaining Wall Design

Wang Qingbiao[1,2,3], Zhang Cong[2], Wang Tiantian[1], Bai Yun[1], LÜ Rongshan[1], Xu Lei[1], Zhang Junxian[1], Hu Zhongjing[1], Xie Fei[1], Zheng Tao[1], Chen Zhen[1], Tang Lingyu[1] and Wang Hui[1,*]

[1]*Department of Resource and Civil Engineering, Shandong University of Science and Technology, Tai'an Shandong 271019, P.R. China;* [2]*State Key Laboratory of Geomechanics and Geotechnical Engineering，Institute of Rock and Soil Mechanics, Chinese Academy of Sciences, Wuhan 430071, P.R. China;* [3]*Shandong Hualian Mining Co., Ltd., Yi'yuan Shandong 256119, P.R. China*

**Abstract:** The introduction and rise of new geotechnical composite material greatly promote the development of civil engineering construction. Studying the mechanical properties of bidirectional geogrid and determining the reinforced soil retaining wall design calculation based on the friction reinforcement theory provide theoretical basis and research foundation for its application in the practical engineering. The mechanical properties of bidirectional geogrid are analyzed in depth through theoretical analysis, experimental research and numerical simulation. The mechanical property tests in light of different affecting factors are studied and the application of geogrid material in the reinforced soil retaining wall is simulated, thus yielding the conclusions as follows: (1) Study the mechanical properties in different temperature, loading and packing with the help of indoor pullout test and analyze the main factors affecting the mechanical properties of the geogrids in theory. (2) Analyze the reinforced soil retaining wall with friction reinforcement principle. Determine the calculation method of soil pressure and reinforcement and the check formula of the overall stability of the whole wall design and calculate the geogrid reinforced soil retaining wall in theory. (3) Simulate the bidirectional geogrid reinforced soil retaining wall with FLAC$^{3D}$and analyze the force of the retaining wall. Study the stress-strain curve according to the parameters of reinforced geogrid and retaining wall and analyze the overall force to guide the safety of the site construction. (4) Apply to the reinforced soil the retaining wall design. Thus the result is achieved that bidirectional geogrid is simple in construction, excellent in performance and economic in cost and has a good application prospect and social benefit.

**Keywords:** Bidirectional geogrid, design calculation, FLAC$^{3D}$, mechanical property, reinforced soil retaining wall.

## 1. INTRODUCTION

The technique of reinforced soil retaining wall is the key technique to solve the high embankment and the stability of high steep slope. With the rise of new composite materials, the geogrid as reinforced material, has gradually become an important part of the reinforced soil retaining wall because of its high tensile, tear resistance, abrasion resistance, chemical resistance, good permeability and friction mosaic [1, 2]. It plays an important role in solving the problem of differential settlement and improving the overall stability. However, there are various kinds of geogrids and the design concept of the current reinforced soil retaining wall is imperfect and only a few kinds of geogrid reinforcement materials are studied [3-5]. So it is necessary to have an in-depth research of geogrid's mechanical properties and its application in reinforced soil retaining wall.

Earlier, the research on geosynthetics was conducted abroad, and its theoretical study and engineering application have been relatively perfect [6-8]. The domestic researches on the new geosynthetics are as follows: Zheng Yingren and Tang Xiaosong [9, 10] studied the stability of high embankment engineering, established the design theory with finite elements and conducted test verification. Xiao Chengzhi and Liu Bo [11] studied the reinforced soil retaining wall with cohesive soil as its filler and analyzed its stress state after long-term testing and monitoring. Cheng Yanan and Sun Shulin [12] studied the reinforced soil retaining wall under bidirectional earthquake force and summarized the calculation formula of the reinforcement material tension and the critical value of the rupture angle from the angle of earthquake disaster. Chen Jianfeng and Liu Junxiu [13] established the model to simulate the field monitoring and deduced the relationship between the stability and the length and layers of reinforcement with finite element analysis. Hu Yun and Zhang Ga [14] established the centrifuge model to conduct the field test and obtained the function of the reinforced belt with the aid of the reinforcement reinforcing mechanism. Peng Fangle and Cao Yanbo [15] studied the shingle and determined the relation curve of the settlement and foundation base pressure of reinforced soil retaining wall with the combination of finite element and indoor experiments. In addition, Shi Danda, Liu Wenbai, Yang Xijie and Wang Shiyue [16-19] conducted research on the reinforced soil retaining wall from different angles and achieved certain results.

*Address correspondence to this author at the Department of Resource and Civil Engineering, Shandong University of Science and Technology, No 223, Daizong Street, Taishan District, Tai'an Shandong 271019, P.R. China; Tel: +86 18805381111; E-mail: 1349725165@qq.com

1874-8368/15 

However, most of the researches presented above studied the specific applications and mechanical properties of geogrid and the design of reinforced retaining wall to a somewhat little extent. There are many types of geogrids and some of them only regard geogrid as reinforced material in micro, but the geotextile, geotechnical composite material and geotechnical specialty material are confused in the construction. Although some of them analyze the influencing factors of geogrid, many parameters need to be controlled and the final effect curve is relatively complex, thus the guiding effect of engineering is poor. Some of the researches only focus on the properties of geogrid and geotextile as well as the advantages as reinforced materials, lacking scientific and reasonable comparative study [20].

On the basis of above account the geogrids are compared in detail in this paper. The mechanical properties of bidirectional geogrid are studied in depth and the design concept and application of reinforced soil retaining wall are explored which have important guiding significance to speed up the popularization and application of new-type of geotechnical composite material and improve engineering benefits.

## 2. MECHANICAL PROPERTIES OF BIDIRECTIONAL GEOGRID

### 2.1. Overview

Bidirectional geogrid is made of high molecular polymer which was extruded, formed and punched and then stretched in the vertical direction of the length on the basis of unidirectional tensile geogrid. It can interact with aging proof agent, acid-resisting material and oxidation-resistant agent to maintain good properties as aging resistance, corrosion resistance and chemical resistance [21]. The structure is shown in Fig. (**1**).

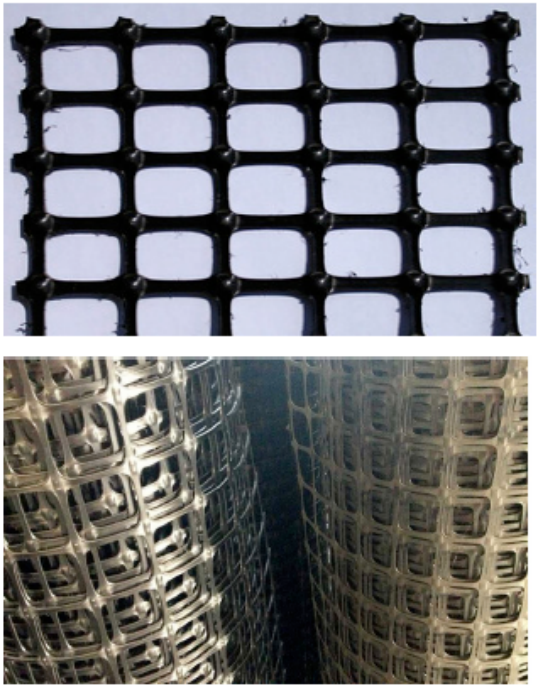

**Fig. (1).** Bidirectional geogrid.

### 2.2. The Analysis of Mechanical Properties

#### *2.2.1. Mechanical Properties*

In the course of design and construction, because the load is different, its mechanical performance evaluation indexes are not the same. The mechanical properties of bidirectional geogrid mainly include the tensile strength, the frictional test strength, pullout test strength and the interaction of fillers.

##### *2.2.1.1. The Tensile Strength*

The bidirectional geogrid is a flexible material, which withstands the load through the tensile strength, thus the tensile strength and its strain are the main characteristic indexes of geosynthetics. The main performance parameters include the longitudinal and transverse tensile strength as much greater than 50kN/m, the longitudinal and transverse elongation as not more than 13% and the tensile strength as far greater than 35kN/m when the elongation is 5%.

##### *2.2.1.2. Creep Characteristic*

The modulus of geogrid is lower while the creep is higher. When it is used as a reinforcement material to calculate the reinforced soil retaining wall stress, in addition to considering the instant stress, the plastic deformation should also be included in the control indexes. The stress and deformation of the geogrid are controlled to assess the safety of reinforced soil retaining wall. So the deformation of reinforced soil retaining wall before the backfill consolidation must be controlled in the allowable range.

##### *2.2.1.3. The Frictional Test Strength*

Bidirectional geogrid is a reticular structure which has longitudinal and transverse cross and the mechanical interlocking formed with the filler, thus it can endure the load under different conditions, having higher bearing capacity and better load transfer performance and less deformation which can prevent the occurrence of dislocation, loosing and separation and the direction can be arbitrarily chosen [22].

In addition, in the process of making bidirectional geogrid, the addition of chemical reagents greatly improved the ageing resistance and chemical resistance properties of geogrid.

## 3. MECHANICAL PROPERTY TEST

Considering that in the process of engineering applications, under different temperature, load and fillers, the tensile properties shown in the geogrid are not the same. So the comparison pullout experiment of unidirectional and bidirectional geogrid is conducted to study the strength properties of bidirectional geogrid.

### 3.1. Test Preparation

The soil samples used in the test involve clay and sand whose parameters are shown in Tables **1**, **2**. The test instruments are TZY-1 new geotechnical material tester which is made by a well-known enterprise and MGT1000 geotechnical material tensile property tester. The geogrids used in the test are TGDG300 unidirectional geogrid and TGSG5050 bidirectional geogrid made by Tai'an Luther Company.

**Table 1. Physical indexes of cohesive soil**

**(1-1)**

| Index | Density | Moisture | Cohesion | Inner friction angle | Plastic limit | Liquid limit |
|---|---|---|---|---|---|---|
| **Numerical value** | 1.85 | 14.7% | 25.7 | 15.3 | 16 | 27 |

**(1-2)**

| Index | Poisson's ratio | Modulus of elasticity | Bulk modulus | Shear modulus | Coefficient of lateral pressure at rest |
|---|---|---|---|---|---|
| **Numerical value** | 0.42 | 5 | 10.4 | 1.76 | 0. 52 |

**Table 2. Physical indexes of sandy soil.**

**(2-1)**

| Index | Density | Moisture | Cohesion | Poisson's ratio |
|---|---|---|---|---|
| Numerical value | 1.56 | 5.7% | 0 | 0.3 |

**(2-2)**

| Index | Modulus of elasticity | Bulk modulus | Shear modulus | Coefficient of lateral pressure at rest |
|---|---|---|---|---|
| Numerical value | 15 | 12.5 | 5.8 | 0.45 |

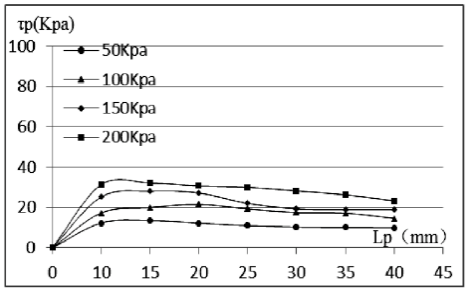


**Fig. (2).** Lp-τp curve diagram(Unidirectional geogrid /Cohesive soil).

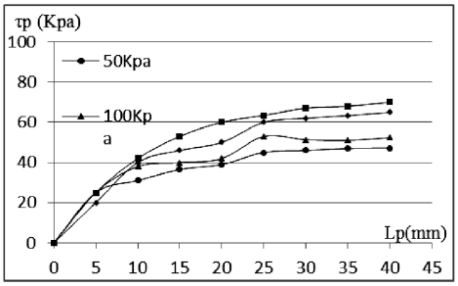


**Fig. (3).** Lp-τp curve diagram(Bidirectional geogrid /Cohesive soil).

### 3.2. Test Method

The comparison pullout test is conducted between unidirectional and bidirectional geogrids. Test device is the composite one shown in document [16] and the soil samples are compacted and consolidated according to the corresponding requirements. In the first group test, the pullout test is taken by applying different loads to the two devices respectively at constant temperature. Strain control is used to conduct the pullout test and employ the same pullout rate, and then record the horizontal force $F$ and displacement $L$ automatically. When L reaches 40mm, the test is stopped. In the second group test, the load is constant and the pullout test is taken under different temperatures and the results are recorded with the tester automatically.

### 3.3. Analysis of Test Results

#### *3.3.1. The Comparison of Pullout Test under Different Loading Conditions*

According to the data recorded automatically by the tester, the pullout test curve is drawn and the pullout test of unidirectional and bidirectional geogrid under different loads is analyzed, obtaining the following:

(1) As is shown in Tables **2** and **3**, when the filler is the same, with the increase of $\tau_p$, the displacement peak appears whether it is unidirectional geogrid or bidirectional one. The displacement of unidirectional geogrid is smaller when the peak appears while the displacement of bidirectional geogrid is larger. Bidirectional geogrid needs larger $\tau_p$ than the unidirectional one to reach the same pullout displacement. This is mainly because the friction occurs between the geogrid and the filler and the interface shear stress of the interlocking force occurs between the grid spacing and the filler. The pore area of the unidirectional geogrid is smaller and the friction plays an important role in the whole process of pullout. The longitudinal and transverse pores of the bidirectional geogrid are larger and the friction is smaller than the interlocking force which ensures the overall strong cohesion and stability.

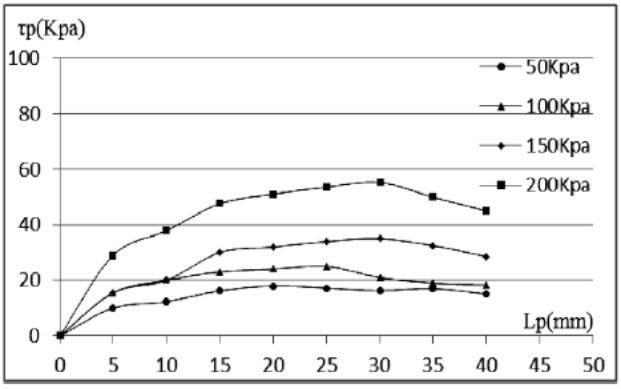


**Fig. (4).** Lp-τp curve diagram (Unidirectional geogrid /Sandy soil).

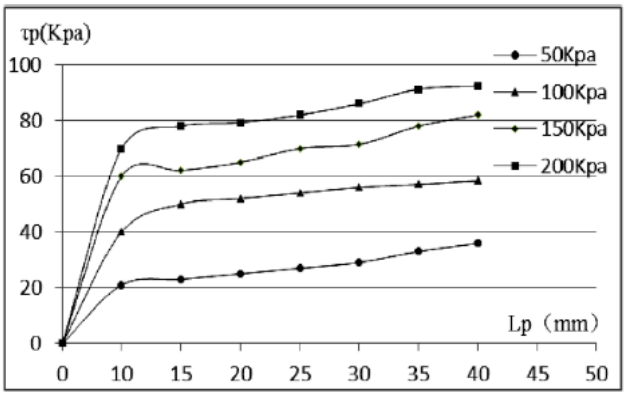


**Fig. (5).** Lp-τp curve diagram (Bidirectional geogrid /Sandy soil).

(2) As is shown in the comparison between Figs. (**2-5**), when the geogrid is the same, the filler also has the effect on the performance of geogrid. The cohesion of the sand is small, but the friction between the particles is more than that of the clay, and the interface friction angle is relatively larger in the pullout test. For clay, the vertical stress has an effect on the interface shear stress peak value and the peak displacement level. For sand, the vertical stress is proportional to the interface shear stress peak value.

### *3.3.2. The Comparison of the Pullout Test under Different Temperatures*

Temperature is one of the main factors affecting the mechanical test. Temperature is prescribed in the current national standard, so the mechanical pullout test is conducted with the temperature as variable parameter. Table **3** shows the mechanical test results under different temperatures. Fig. (**6**) represents the strain-time diagram at different temperatures and when the stress level is 40%. The abscissa is the index with base 10.

Based on the test data analysis, temperature has a larger effect on the bidirectional geogrid. With the increase in the temperature, the strain value increases gradually. Bidirectional geogrid as reinforced material used in engineering, the case at 60℃can be ignored considering the actual situation. As is shown in Fig. (**6**), the higher is the temperature, the larger is the strain of the geogrid with the change of time. From Table **3**, it can be seen that in a certain temperature range, the tensile strength of bidirectional geogrid reaches the maximum value of 137.05 kN/m at 16°C. With the increase n the temperature, the strength decreases to 115.94 kN/m when the temperature is 30°C, which is basically a linear relationship. Nominal elongation is only 9.39% at 16°C. With the increase in the temperature, the nominal elongation becomes larger gradually and reaches 10.21% at 30°C which is positively correlated.

**Table 3. Test of bidirectional geogrid under different temperatures.**

**(3-1)**

| Temperature (℃) | 16 | 18 | 20 | 22 |
|---|---|---|---|---|
| Tensile strength (kN/m) | 137.05 | 133.61 | 129.06 | 128.11 |
| Nominal elongation (%) | 9.39 | 9.45 | 9.70 | 9.83 |

**(3-2)**

| Temperature (℃) | 24 | 26 | 28 | 30 |
|---|---|---|---|---|
| Tensile strength (kN/m) | 126.95 | 124.14 | 120.152 | 115.94 |
| Nominal elongation (%) | 9.92 | 9.97 | 10.10 | 10.21 |

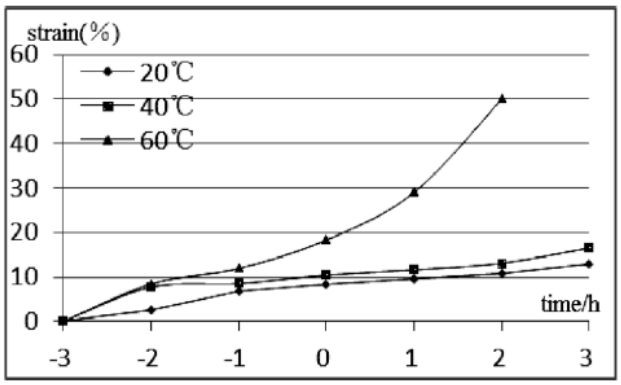


**Fig. (6).** The strain - time curve (Different temperature conditions).

## 4. BIDIRECTIONAL GEOGRID REINFORCED SOIL RETAINING WALL DESIGN CALCULATION

### 4.1. Principle of Reinforcement

Bidirectional geogrid reinforced soil retaining wall is composed of the wall shingle, reinforced materials (bidirectional geogrid) and the filler. Bidirectional geogrid is embedded in soil along the strain direction, depending on the friction resistance and cohesion between the soil and geogrid to modify the mechanical properties of soil. The weight of the earth-fill and the external force act on the wall shingle, transfer the soil pressure to the reinforcement through the reinforcement connections of wall shingle and ensure the

stability of geogrid under the action of the friction between soil and geogrid. Bidirectional geogrid has greater tensile strength and the grid structure forms friction resistance with the earth-fill to ensure the stability of reinforced soil.

### 4.2. The Calculation of Earth Pressure

#### *4.2.1. The Calculation of Lateral Earth Pressure*

The earth pressure caused by the backfill $s_s = \psi_s \sum_{i=1}^{n} \lambda_{si} \Delta w_i h_i$

and the earth pressure caused by the load of the top of the wall

$$\Delta w_i = \Delta w_1 - (\Delta w_1 - 0.01)\frac{z_{i-1}}{z_{n-1}}$$

composed of the lateral earth pressure on the wall shingle $p$.

(1) The calculation of $\Delta w_1 = w_1 - \phi_w w_p$

The earth pressure caused by the backfill

$$s_s = \psi_s \sum_{i=1}^{n} \lambda_{si} \Delta w_i h_i$$

is close to the earth pressure at rest, and the calculation formula is

$$p_1 = K_0 \cdot \gamma \cdot h_i \quad (1)$$

In it: $K_0$——the earth pressure at rest coefficient of earth-fill, $k_0 = 1 - \sin\varphi$ ;

$h_i$——the range of the action point of earth pressure, $h_i \le H/2$, $h_i$ is the actual value, $h_i$ is 0.5H ;

(2) The calculation of $p_2$

The value of the earth pressure caused by load $P_2$ is inversely proportional to the distance between the wall shingle and the top of the wall. The most convenient method is to

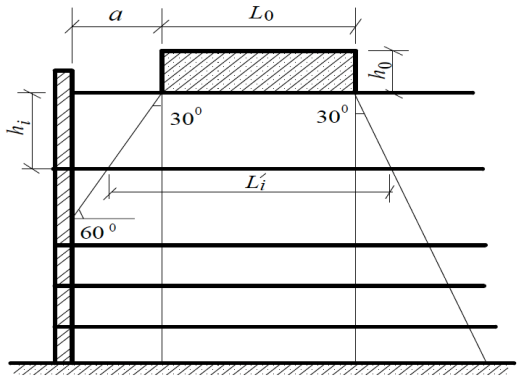


**Fig. (7).** Load diffusion angle method.

obtain the value of $P_2$ by the product of the vertical earth pressure caused by load and the coefficient of earth pressure at rest. Using soil mechanics stress diffusion, angle method to calculate the vertical earth pressure strength and the diffusion angle of the earth-fill is $30^0$ as is shown in Fig. (**7**)

The calculation formula is:

$$p_2 = K_0 \cdot \frac{\gamma \cdot h_0 \cdot L_0}{L_i'} \quad (2)$$

In it:

$L_0$——the equivalent width of the soil column ;

$h_0$——the equivalent height of the soil column ;

$\gamma$——load converted into the weight of the earth-fill ;

$a$——the shortest distance between the load and the inside of the wall shingle ;

$L_i'$——the diffusion width of the load ;

When $h_i \le a \cdot \tan 60°$, $L_i' = L_0 + 2h_i \cdot \tan 30°$ ;

When $h_i > a \cdot \tan 60°$, $L_i' = a + L_0 + h_i \cdot \tan 30°$.

#### *4.2.2 The Calculation of Vertical Pressure*

The calculation formula of the vertical pressure value acting on the location of the $i$ layer reinforcement is:

$$q_i = q_1 + q_2 = \gamma \cdot h_i + \gamma . h_0 L_0 / L_i' \quad (3)$$

### 4.3. The Calculation of Reinforcement

(1) The design value of tensile force of reinforcement $T_i$

Under the action of the active earth pressure, single reinforcement force should be balanced with the lateral earth pressure of the wall shingle, that is:

$$T_i = K \cdot p_i \cdot S_x \cdot S_y \quad (4)$$

In it:

$T_i$——the design value of tensile force of reinforcement of the $i$ layer (kN).

$p_i$——the lateral earth pressure value of the wall shingle at the corresponding reinforcement (Kpa), $p_i = p_{i1} + p_{i2}$.

$S_x$——the horizontal spacing of reinforcement(m).

$S_y$——the vertical spacing of reinforcement (m).

$K$——safety coefficient, usually $K = 1.5 \sim 2.0$ .

According to the above that the pulling force of the single reinforcement is proportional to the depth of the earth-fill and the maximum tensile force appears at the bottom reinforcement. The maximum tensile stress of each reinforcement $\sigma_{max}$ is in the interface of sliding zone and anchorage zone, which is acting on the surface of the fracture. The tensile stress of the connections between reinforcement and wall shingle is approximately equal to 0.75 times of the maximum tensile stress.

(2) The resistance of the earth-fill to the reinforcement $T_b$

Because the reinforcement is under the action of the vertical earth pressure, the pulling resistance of the reinforcement is produced (or it is called anchoring force), that is:

$$T_b = 2\mu \cdot q_i \cdot b \cdot L_e \quad (5)$$

In it:

$T_b$ ——the pulling resistance of the reinforcement in the anchorage zone (kN).

$\mu$ ——the friction coefficient of the earth-fill and reinforcement, sand soil $\mu = 0.35 \sim 0.5$ .clay soil $\mu = 0.25 \sim 0.4$.

$b$ ——reinforcement width(m).

$L_e$ ——the effective length of the reinforcement(m).

$q_i$ ——the vertical pressure value of the actual location of the $i$ layer of reinforcement(Kpa).

(3) The effective length of the reinforcement $L_e$

According to the force balance of the reinforcement $T_i = T_b$ can get:

$$L_e = \frac{T_i}{2\mu \cdot q_i \cdot b} \quad (6)$$

(4)The invalid length of reinforcement $L_0$

The invalid length of reinforcement is determined with the $0.3H$ polygon method,

When $h_i \le 0.5H$， $L_0 = 0.3H$ ；

When $h_i > 0.5H$， $L_0 = 0.6(H - h_i)$.

(5)The overall length of the reinforcement $L$

In theory, the overall length of the reinforcement

$L = L_0 + L_e$. The construction requirements of reinforced soil retaining wall should be considered in the design. In fact, the overall length of reinforcement$L$ has a certain proportional relation with the height of the retaining wall$H$.

When $H > 3\,\text{m}$， $L_{\min} \ge 0.7H$, and $L_{\min} > 5.0\,\text{m}$. If the unequal reinforcement is used, the short reinforcement $L_{\min} \ge 0.5H$.

When $H \le 3\,\text{m}$， $L_{\min} \ge 4.0\,\text{m}$, the equal reinforcement is used.

(6)The sectional area of reinforcement $A$

When the pulling design value of the reinforcement $T_i$ is fixed, the sectional area of reinforcement $A$ is certain according to the design value of the tensile strength of reinforcement material $f_y$, that is:

$$A \ge T_i / f_y \quad (7)$$

For steel reinforcement, in addition to meet the computing requirements, steel corrosion and the requirements of tensile strength of reinforcement joints should also be considered. For the reinforced concrete reinforcement, to calculate the center tensile member, the steel diameter can be obtained after adding 2mm to it. To prevent concrete fracturing, the stirrup or crack resistant should be placed in the reinforcement plate. For polypropylene geobelt reinforcement, the limit fracture tension value of each geobelt should be tested and the 1/5～1/7of the value should be taken as the design value of tensile strength.

### 4.4. The Calculation of the Overall Stability of the Whole Wall

Reinforced soil retaining wall adopts the designing method of gravity retaining wall to check the sliding stability and the anti-overturning stability of the whole wall and the foundation bearing capacity. The calculation formula of the overall stability of the whole wall is as follows:

$$K_b = \sum T_{pi} \Big/ \sum T_i \ge 2 \quad (8)$$

## 5.NUMERICAL SIMULATION ANALYSIS

### 5.1. Model Construction

Based on the geological conditions of the construction of Jiaoqu tunnel section Taixing railway, FLAC$^{3D}$ is used to carry out the three-dimensional numerical simulation of reinforced soil retaining wall.Three layers of bidirectional geogrid are distributed in the reinforced geogrid of the retaining wall with the spacing of 0.5m and 20 layers altogether. Seven layers of 9m geogrid are arranged in the middle and six layers of 8m geogrid are arranged on the top and bottom respectively.The model consists of 66000 units and 71791nodes as shown in Fig. (**8**).

In addition, the experiment is carried out under the time taken to get in balance. The temperature of the surface rotor begins to decrease with the experimental time, and at last the temperature is balanced. During the process, it takes about 22 minutes for different rotation speeds.

### 5.2. Parameter Setting

Mohr-Coulomb Model is used inthe earth-fill in the retaining wall model and bidirectional geogrid. The density $\rho$, modulus of elasticity E, shear modulus G, bulk modulus K and Poisson's ratio ν are all obtained from the calculation of the field test indexes. The parameters of backfill, bidirectional geogrid and precast retaining wall are mentionedin Table **4**.

### 5.3.The Analysis of Calculation Results

According to the numerical simulation results of retaining wall, the stress-strain simulated nephogram in X and Z direction and the stress-strain relation curve of retaining wall are analyzed. Figs. (**9** and **10**) show the stress nephogram of retaining wall in X and Z direction.

**Table 4. Summary of model parameters.**

| Parameters test content | Density $\rho$/g.cm$^3$ | Cohesion c/Kpa | Internal friction angle$\varphi$($^o$) | Poiss-on's ratio v | Modulus of elasticity E/Mpa |
|---|---|---|---|---|---|
| **geogrid** | 19 | 0 | 0 | 0.21 | 650 |
| **Grid filler** | 22 | 16 | 27.6 | 0.22 | 25 |
| **Wall shingle (C25concrete)** | 25 | 0 | 0 | 0.23 | 8000 |
| **The rear filler of geogrid** | 20 | 10.3 | 27.6 | 0.22 | 25 |
| **Foundation soil** | 22 | 14.6 | 27.9 | 0.24 | 25 |

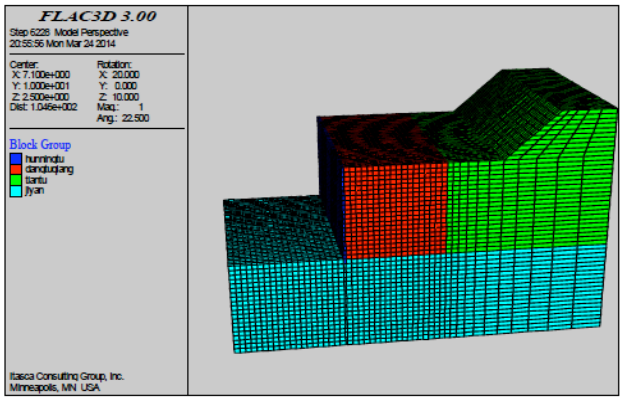


**Fig. (8).** The schematic diagram of bidirectional geogrid reinforced soil retaining wall model.

Fig. (**11**) represents the strain nephogram of retaining wall along Z direction. Fig. (**12**) is the stress-strain curve with the increase in steps.

From the analysis of the stress nephogram of retaining wall in X direction, the top stress of the retaining wall and the filler is greater and the maximum is $2.16\times10^5$ N/m$^2$. The biggest change appears at the top of the slope, and the stress in X direction gradually decreases to zero along with the increase in buried depth. From the stress nephogram, it can be observed that the stress change of the reinforced retaining wall in X direction meets the design requirements.

From Figs. (**10** and **11**), it is shown that the stress value of the retaining wall along Z direction reaches the maximum at the top of the hill which is $4.13\times10^5$ N/m$^2$ by means of numerical simulation. The stress value in the vertical direction decreases gradually with the increase in depth mainly due to the gravity of the retaining wall and the filler. The strain along the Z direction reduces gradually. From the strain nephogram,it can be seen that the interlocking between geogrid and the filler is significant after reinforcement and the overall stability is enhanced. Simulation results show that the maximum displacement is $3\times10^2$m which meets the requirements of standard design.

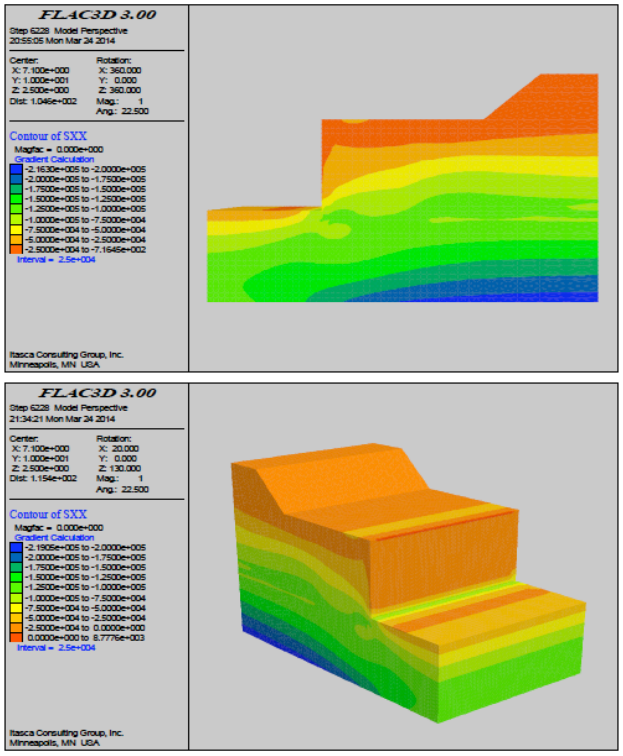


**Fig. (9).** Stress nephogram of retaining wall in X direction.

According to the numerical simulation,the displacement of the top of the slope and the top of the interface of the retaining wall and the filler is analyzed. From Fig. (**12**), it can be seen that with the progress of the project, the strain increases gradually and there is a linear relationship in the antecedent strain.Under the interaction of wall shingle, bidirectionalgeogrid and filler, the strain growth rate in the vertical direction slows down gradually and the two maximum values are $3.5\times10^{-2}$m and $7.8\times10^{-3}$m. The strain decreases and gradually maintains steady state after the peak,meeting the design requirements.

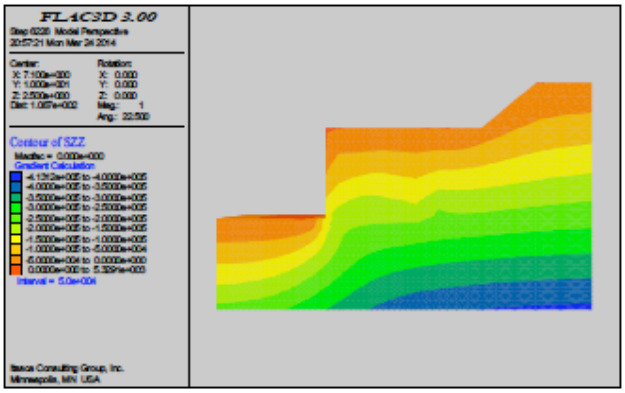


**Fig. (10).** Stress nephogram of retaining wall in Z direction.

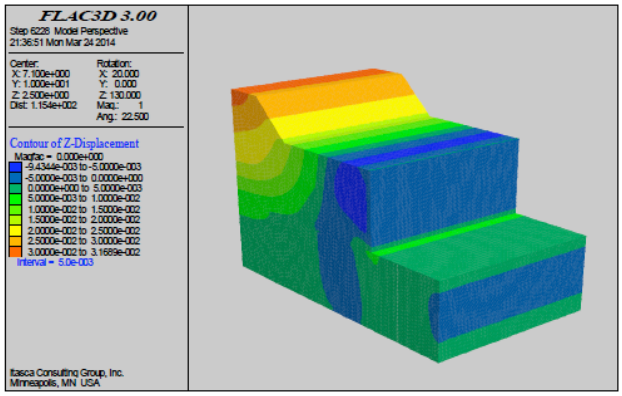


**Fig. (11).** Stress nephogram of retaining wall along Z direction.

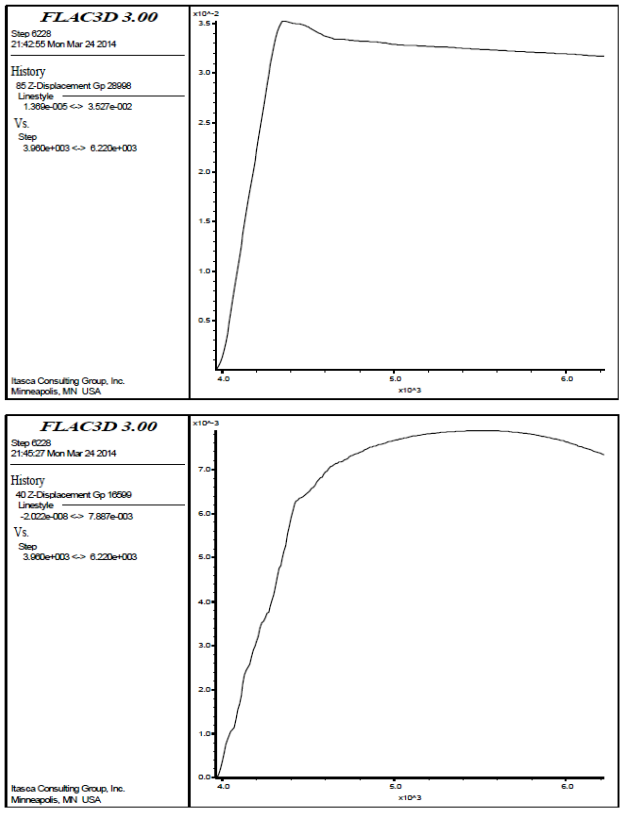


**Fig. (12).** The stress-strain curve with the increase of steps.

To sum up, bidirectional geogridholds great stiffness, high strength and good coordinate deformation capacity. When acting on the reinforced retaining wall as reinforcement material, it can be integrally formed with the filler after compaction to commonly bear and uniformly share loads and limit the lateral deformation of soil. At the same time, tight bidirectional geogrid can reduce the settlement of the soil, so as to ensure the integrity and stability of the retaining wall.

## CONCLUSION

(1) When the geogrid is studied as reinforcement material, the macroscopic analysis of the mechanical properties of geogrid is not enough. There are varieties of geogrids, thus these should be refined to specific one and focus on its mechanical properties. When the indoor test of mechanical properties of geogrid is carried out, the actual situation of engineering should be considered and the pullout test should be conducted on it. Comparative analysis is conducted in different temperatures, under different loads and with different fillers, and this can guide the construction along with the influencing factors in the pullout test curve.

(2) With the help of friction reinforcement theory, calculation formula of lateral earth pressure and vertical pressure and when the parameters are certain, the earth pressure of reinforced soil retaining wall backfill and the top of the wall should be calculated. According to the reinforcement design calculation formula, the tensile design value, resistance between reinforcement and the filler and the length and sectional area of reinforcement are calculated which provide theoretical reference for the subsequent numerical simulation and the practical application in engineering to ensure the safety of the construction.

(3) Numerical simulation isconducted on bidirectional geogrid reinforced retaining wall by FLAC$^{3D}$, and the stress-strain nephogram is drawn with the simulation results which analyze the stress-strain maximum and the change trend fully and intuitively. Combined with the stress-strain curve, the performance of bidirectional geogrid as reinforced material is tested.

(4) With high strength and good coordinate deformation capacity, when acting on the reinforced retaining wall as reinforcement material, bidirectional geogrid can be integrally formed with the filler after compaction to limit the lateral deformation of soil. At the same time, bidirectional geogrid under load can reduce the settlement of the soil, so as to ensure the integrity and stability of the retaining wall. In addition, bidirectional geogrid can be widely used in the national key projects as water conservancy project, railway engineering and soft soil foundation treatment which have wide application prospects and great social and economic benefits.

## CONFLICT OF INTEREST

The authors confirm that this article content has no conflict of interest.

## ACKNOWLEDGEMENTS

This work was financially supported by:

(1) National Natural Science Foundation of China (NSFC) (41372289).

(2) SDUST Research Fund (2014TDJH103).

(3) A Project of Shandong Province Higher Educational Science and Technology Program (12LH03).

(4) China's Post-doctoral Science Fund (2012M521365).

## REFERENCES

[1] Z. Xiaofeng, Z. Mengxi and Q. Chengchun, "Strength of sand reinforced with different forms of geogrid", *Jiaotang Shanghai Jiao Tong University*, vol. 47, pp. 1378-1383, 2013.

[2] Y. Guangqing, Z. Yitao and Z. Qiaoyong, "Distribution rules of axial stress of reinforcement in reinforce dearth retaining wall", *Rock and Soil Mechanics*, vol. 35, pp. 651-655, 2013.

[3] A. T. Özer, O. Akay , G.A. Fox, S.F. Bartlett and D. Arellano, "A new method for remediation of sandy slopes susceptible to seepage flow using EPS-block geofoam". *Geotextiles and Geomembranes*, vol. 42, pp. 166-180, 2014.

[4] V. Toufigh, C. S. Desai, H. Saadatmanesh, V. Toufigh, S. Ahmari and E. Kabiri, "Constitutive modeling and testing of interface between backfill soil and fiber reinforced polymer (CFRP)", *International Journal of Geomechanics*, vol. 14, no. 3, p. 2147483647 2013.

[5] R. P. Chen, Z. Z. Xu, Y. M. Chen, D. S. Ling, and B. Zhu, "Field test research on embankment supported by plastic tube cast-in-place concrete piles", *Geotechnical and Geological Engineering*, vol. 31, pp. 1359-1368, 2013.

[6] L. Lei, Z. Meng-xi and Z. Xiao-feng, "With strengthening node bidirectional geogrid drawing test research", *Journal Of Hydraulic*, vol. 46-48, pp. 1494-1499, 2012.

[7] X. Sifa, H. Qi and W. Zhe, "Experimental study on deformation characteristics of geogrid reinforced cushion system local settlement of foundation", *China Civil Engineering Journal*, vol. 44, pp. 46-49, 2011.

[8] R.D. Hryciw, A. Athanasopoulos-Zekkos and N. Yesiller, "*Geo-Congress 2012: State of the Art and Practice in Geotechnical Engineering*", ASCE GeoCongress: 2012.

[9] H. Brandl, "Geosynthetics applications for the mitigation of natural disasters and for environmental protection", *Geosynthetics International*, vol. 18, pp. 340-390, 2011.

[10] D. Xiaosong, W. Yongfu and Z. Yingren. Geogrid reinforced soil retaining wall discussed several problems should be paid attention to in the design and construction. *Journal of Disaster Prevention and Mitigation Engineering*, vol. 33, pp. 89-94, 2013.

[11] X. Chengzhi, L. Bo and L. Yu-run, "Test study of long-term performances of reinforced cohesion soil retaini", *Rock and Soil Mechanics*, vol. 33, pp. 110-115, 2012.

[12] C. Yanan, S. Shulin and R. Xiaobo, "Pseudo-dynamic analysis of seismic stability of reinforced soil walls", *Rock and Soil Mechanics*, vol. 34, pp. 3573-3579, 2013.

[13] C. Jianfeng, L. Junxiu and S. Zhenming, "Numerical simulation and stability discussion of a reinforced soil retaining wall on soft soil foundation", *Chinese Journal of Rock Mechanics and Engineering*, vol. 31, pp. 1929-1936, 2012.

[14] H. Yun, Z. Ga and L. Wenxing, "Centrifuge modeling of geo textile reinforced cohesive soil slopes under surface loading", *Rock and Soil Mechanics*, vol. 32, pp. 1327-1332, 2011.

[15] P. Lefang and C. Yanbo, "Numerical analysis of effect of facing rigidity on reinforced-sand retaining walls", *Rock and Soil Mechanics*, vol. 33, pp. 865-872, 2012.

[16] S. Dan-da, L. Wen-Bai and S. Wei-Hou, " Single, two-way plastic geogrid with different filler interface function contrast test research", *Rock and Soil Mechanics*, vol. 30, 2009.

[17] Y. Xijie, W. Shiyue and L. Zhengcong, "Evaluation of Influence of Temperature on Mechanical Property of Glassgrid and Uncertainty", *Journal of Highway and Transportation Research and Development*, vol. 26, pp. 45-48, 2009.

[18] J.S. Tingle, G.J. Norwood, S.R. Jersey and J. Kwon, "Full-scale evaluation of geogrid-reinforced thin flexible pavements. Transportation research record", *Journal of the Transportation Research Board*, vol. 2310, pp. 61-71, 2012.

[19] G.R. Chehab and X. Tang, " The use of a multi-set-up, reduced-scale accelerated trafficking simulator for evaluating roadway systems and products", *International Journal of Pavement Engineering*, vol. 13, pp. 535-552, 2012.

[20] L. Ze, H. Xiangjing and Y. Linguo, "Study of a combined panel earth retaining wall reinforced with double twisted hexagonal wire mesh by using site test", *Rock and Soil Mechanics*, vol. 32, pp. 3296-3300, 2011.

[21] C. Jianfeng, L. Junxiu and S. Zhenming, " Three-dimensional Numerical Simulation of a Reinforced Soil Wall", *Journal of Tongji University (Natural Science)*, vol. 33, pp. 2018-2056, 2012.

[22] D. Jinhua, T. Jun and Z. Jing, "Study of influence of environmental factors on geogrid creep property". *Rock and Soil Mechanics*, vol. 33, pp. 2048-2056, 2012.

Received: May 26, 2015 Revised: July 14, 2015 Accepted: August 10, 2015